

Comparative study of the production of scalar and tensor mesons in e^+e^- collisions

N. N. Achasov,^{1,*} A. I. Goncharenko,^{1,2} A. V. Kiselev,^{1,2,†} and E. V. Rogozina^{1,2}

¹Laboratory of Theoretical Physics, Sobolev Institute for Mathematics, 630090 Novosibirsk, Russia

²Novosibirsk State University, 630090 Novosibirsk, Russia

(Received 6 July 2013; published 2 December 2013)

The intensity of scalar $a_0(980)$, $f_0(980)$ and tensor $a_2(1320)$, $f_2(1270)$ mesons production at VEPP-2000 (BINP, Novosibirsk) and the upgraded DAΦNE (Frascati, Italy) in the processes $e^+e^- \rightarrow a_0(f_0, a_2, f_2)\gamma$ is calculated. For the scalar meson production the calculation is performed with the help of the vector dominance model (VDM) and the kaon loop model. Only the VDM approach is used in the tensor meson case. Note that the processes $e^+e^- \rightarrow a_2(f_2)\gamma$ have not been studied in the energy region of VEPP-2000. It turned out that in the VEPP-2000 energy region 1.7–2.0 GeV $\sigma_{e^+e^- \rightarrow a_2(f_2)\gamma} \sim 10$ pb, and $\sigma_{e^+e^- \rightarrow a_0(f_0)\gamma} \sim 0.1$ pb. Photon angle distribution and the spin density matrices of a_2 and f_2 production are also calculated.

DOI: 10.1103/PhysRevD.88.114001

PACS numbers: 12.39.-x, 13.40.Hq, 13.66.Bc

I. INTRODUCTION

Study of the nature of light scalar resonances is one of the central problems of nonperturbative QCD, it is important for understanding the way chiral symmetry is realized in the low energy region and, consequently, for the understanding of confinement. The $a_2(1320)$ and $f_2(1270)$ tensor mesons are well-known P-wave $q\bar{q}$ states. Naively one might think that the scalar $a_0(980)$ and $f_0(980)$ mesons are also the $q\bar{q}$ P-wave states with the same quark structure, as $a_2(1320)$ and $f_2(1270)$, respectively. But now there are many indications that the above scalars are four quark states.

Comparative study of the production of scalar and tensor mesons is proposed to investigate the nature of light scalar mesons. For this purpose the intensity of scalar $a_0(980)$, $f_0(980)$ and tensor $a_2(1320)$, $f_2(1270)$ mesons production at the colliders VEPP-2000 (BINP, Novosibirsk) and DAΦNE (LNF, Frascati) in the processes $e^+e^- \rightarrow S\gamma$, $T\gamma$ (here and hereafter $S = a_0, f_0$; $T = a_2, f_2$) is calculated.

The formulas for the reactions $e^+e^- \rightarrow a_0(f_0)\gamma \rightarrow \eta(\pi^0)\pi^0\gamma$ are given in Sec. II. Results for the reactions $e^+e^- \rightarrow a_2(f_2)\gamma$ including $\eta\pi^0$ and $\pi^0\pi^0$ mass spectra are presented in Sec. III. The background situation is discussed in Sec. IV, and a brief summary is given in Sec. V.

II. THE REACTIONS $e^+e^- \rightarrow a_0\gamma \rightarrow \eta\pi^0\gamma$ AND $e^+e^- \rightarrow f_0\gamma \rightarrow \pi^0\pi^0\gamma$

As it is known, the kaon loop model [1,2] describes the $V \rightarrow K^+K^- \rightarrow a_0(f_0)\gamma$ decays well [3–11]. The signal contribution is $e^+e^- \rightarrow \sum_V V \rightarrow K^+K^- \rightarrow a_0(f_0)\gamma \rightarrow \eta(\pi^0)\pi^0\gamma$, where V are vector mesons. The signal cross sections are

$$\begin{aligned} \frac{d\sigma_{e^+e^- \rightarrow a_0\gamma \rightarrow \eta\pi^0\gamma}(s, m)}{dm} &= \frac{g_{a_0\eta\pi^0}^2 P_{\eta\pi}(m)}{4\pi^2 |D_{a_0}(m)|^2} \sigma_{e^+e^- \rightarrow a_0\gamma}(s, m) \\ &= \frac{e^4 (s - m^2) P_{\eta\pi}(m)}{96\pi^3 s^3} |A_{K^+K^-}(s) \bar{g}(m)|^2 \left| \frac{g_{a_0K^+K^-} g_{a_0\eta\pi^0}}{D_{a_0}(m)} \right|^2, \end{aligned} \quad (1)$$

$$\begin{aligned} \frac{d\sigma_{e^+e^- \rightarrow f_0\gamma \rightarrow \pi^0\pi^0\gamma}(s, m)}{dm} &= \frac{g_{f_0\pi^0\pi^0}^2 P_{\pi\pi}(m)}{4\pi^2 |D_{f_0}(m)|^2} \sigma_{e^+e^- \rightarrow f_0\gamma}(s, m) \\ &= \frac{e^4 (s - m^2) P_{\pi\pi}(m)}{96\pi^3 s^3} |A_{K^+K^-}(s) \bar{g}(m)|^2 \left| \frac{g_{f_0K^+K^-} g_{f_0\pi^0\pi^0}}{D_{f_0}(m)} \right|^2, \end{aligned} \quad (2)$$

$$P_{\eta\pi}(m) = \frac{\sqrt{(m^2 - (m_\eta + m_\pi)^2)(m^2 - (m_\eta - m_\pi)^2)}}{2m},$$

$$P_{\pi\pi}(m) = \frac{\sqrt{m^2 - 4m_\pi^2}}{2}.$$

The $A_{K^+K^-}(s)$ is the amplitude of the $\gamma^* \rightarrow K^+K^-$ transition. Without mixing of the intermediate vector states this amplitude is

$$A_{K^+K^-}(s) = \sum_{V=\rho, \rho', \rho'', \omega, \omega', \omega'', \phi, \phi', \phi''} \frac{g_{V\gamma} g_{VK^+K^-}}{D_V(s)}, \quad (3)$$

where, as usual, $\rho = \rho(770)$, $\rho' = \rho(1450)$, $\rho'' = \rho(1700)$, $\omega = \omega(782)$, $\omega' = \omega(1420)$, $\omega'' = \omega(1650)$, $\phi = \phi(1020)$, $\phi' = \phi(1680)$, $\phi'' = \phi(2170)$. We took into account mixing of the resonances according to Ref. [12]. The s is the e^+e^- total energy squared, m is the $\eta\pi^0$ or $\pi^0\pi^0$ invariant mass correspondingly, $g_{V\gamma} = em_V^2/f_V$, $g_{f_0\pi^0\pi^0} = g_{f_0\pi^+\pi^-}/\sqrt{2}$ for the pions

*achasov@math.nsc.ru

†kiselev@math.nsc.ru

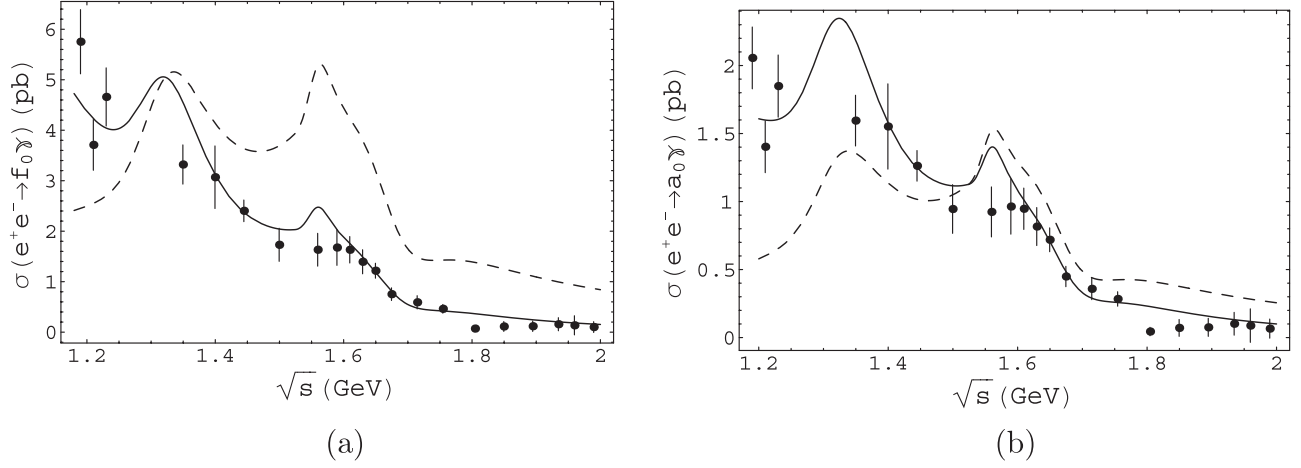


FIG. 1. The (a) $\sigma_{e^+e^- \rightarrow f_0\gamma}(s, m = m_{f_0})$ and (b) $\sigma_{e^+e^- \rightarrow a_0\gamma}(s, m = m_{a_0})$. Solid lines show the kaon loop model prediction, dashed lines show 1/10 of the cross sections in case of the mere VDM prediction for the pointlike $VS\gamma$ interaction normalized on the signal at $\sqrt{s} = m_\phi$. Points are the result of using the experimental data [14,15] on the $\sigma_{e^+e^- \rightarrow K^+K^-}(s)$ in Eqs. (4) and (5).

identity, and $\bar{g}(m) = \frac{g_R(m)}{e g_{\phi K^+ K^-} - g_{RK^+ K^-}}$ is the integral on the kaon loop [1]. The $D_{a_0}(m)$ and $D_{f_0}(m)$ are the inverse propagators of scalar mesons; they may be taken from [9,11] (2012 paper) correspondingly. In this paper we use only $m_{a_0} = 1003$ MeV, $g_{a_0 K^+ K^-}^2/4\pi = 0.82$ GeV² and $m_{f_0} = 978.3$ MeV, $g_{f_0 K^+ K^-}^2/4\pi = 1$ GeV². The Eqs. (1) and (2) may be rewritten as

$$\begin{aligned} \frac{d\sigma_{e^+e^- \rightarrow a_0\gamma \rightarrow \eta\pi^0\gamma}(s, m)}{dm} &= \frac{e^2(s-m^2)p_{\eta\pi}(m)}{2\pi^2\sqrt{s}(s-4m_{K^+}^2)^{3/2}} |\bar{g}(m)|^2 \left| \frac{g_{a_0 K^+ K^-} g_{a_0 \eta\pi^0}}{D_{a_0}(m)} \right|^2 \\ &\times \sigma_{e^+e^- \rightarrow K^+K^-}(s), \end{aligned} \quad (4)$$

$$\begin{aligned} \frac{d\sigma_{e^+e^- \rightarrow f_0\gamma \rightarrow \pi^0\pi^0\gamma}(s, m)}{dm} &= \frac{e^2(s-m^2)p_{\pi\pi}(m)}{2\pi^2\sqrt{s}(s-4m_{K^+}^2)^{3/2}} |\bar{g}(m)|^2 \left| \frac{g_{f_0 K^+ K^-} g_{f_0 \pi^0\pi^0}}{D_{f_0}(m)} \right|^2 \\ &\times \sigma_{e^+e^- \rightarrow K^+K^-}(s). \end{aligned} \quad (5)$$

After integration over m one obtains the cross sections $\sigma_{e^+e^- \rightarrow a_0\gamma \rightarrow \eta\pi^0\gamma}(s)$ and $\sigma_{e^+e^- \rightarrow f_0\gamma \rightarrow \pi^0\pi^0\gamma}(s)$. The photon angular distribution is

$$\frac{dn_\gamma^S}{d\Omega} = \frac{3}{16\pi} (1 + \cos^2\theta), \quad (6)$$

where θ is the angle between the γ momentum and the beam axis.

In Fig. 1 we show the $\sigma_{e^+e^- \rightarrow K^+K^- \rightarrow S\gamma}(s, m = m_S)$ cross-sections prediction, the mere vector dominance model (VDM) one (pointlike $VS\gamma$ interaction) is shown also [13]. Points on Fig. 1 are obtained with the help of the experimental data [14,15] on the $e^+e^- \rightarrow K^+K^-$ and Eqs. (1), (2), (4), and (5). Curves are drawn with the vector

meson parameters close to the Ref. [12] ones. Note that $\sigma_{e^+e^- \rightarrow a_0\gamma \rightarrow \eta\pi^0\gamma}(s)$ and $\sigma_{e^+e^- \rightarrow f_0\gamma \rightarrow \pi^0\pi^0\gamma}(s)$ are less than $\sigma_{e^+e^- \rightarrow K^+K^- \rightarrow a_0\gamma}(s, m = m_{a_0})$ and $\sigma_{e^+e^- \rightarrow K^+K^- \rightarrow f_0\gamma}(s, m = m_{f_0})$ correspondingly for the branching fractions ($B(f_0 \rightarrow \pi^0\pi^0) = 1/3 B(f_0 \rightarrow \pi\pi) \leq 1/3$) and an extraction of the a_0 and f_0 resonance regions in the mass spectra, usually made by experimentalists.

Note also that the vector dominance model describes form factors (and transition form factors) of $q\bar{q}$ states in the low and intermediate energy regions. In the case of the four quark states $S = a_0, f_0$ the amplitude of the process $\gamma^* \rightarrow S\gamma$ along with VDM suppression $(m_V^2 - s)^{-1}$ has also additional suppression $\frac{(2m_K)^2}{s} \ln^2 \frac{s}{m_K^2}$ with increasing s for the kaon loop, see Eq. (12) in [16]. This provides additional suppression in comparison with the $q\bar{q}$ state case, see Fig. 1.

III. THE REACTION $e^+e^- \rightarrow a_2(f_2)\gamma$

It is known that in the reaction $\gamma\gamma \rightarrow f_2 \rightarrow \pi\pi$ tensor mesons are produced mainly by the photons with the opposite helicity states. The effective Lagrangian in this case is

$$L = g_{f_2\gamma\gamma} T_{\mu\nu} F_{\mu\sigma} F_{\nu\sigma}, \quad F_{\mu\sigma} = \partial_\mu A_\sigma - \partial_\sigma A_\mu, \quad (7)$$

where A_μ is a photon field and $T_{\mu\nu}$ is a tensor f_2 field. So in the frame of the vector dominance model we assume that the effective Lagrangian of the reaction $f_2 \rightarrow VV$ is [17]

$$L = g_{f_2VV} T_{\mu\nu} F_{\mu\sigma}^V F_{\nu\sigma}^V, \quad F_{\mu\sigma}^V = \partial_\mu V_\sigma - \partial_\sigma V_\mu, \quad (8)$$

where $V = \rho, \rho', \rho''\omega, \omega', \omega''$. Note that ω, ω' and ω'' give $\sim 10\%$ of the ρ, ρ' and ρ'' contribution in the amplitude, so then we neglect them: our current aim is to obtain estimates only. The $\rho - \rho' - \rho''$ mixing is omitted here also.

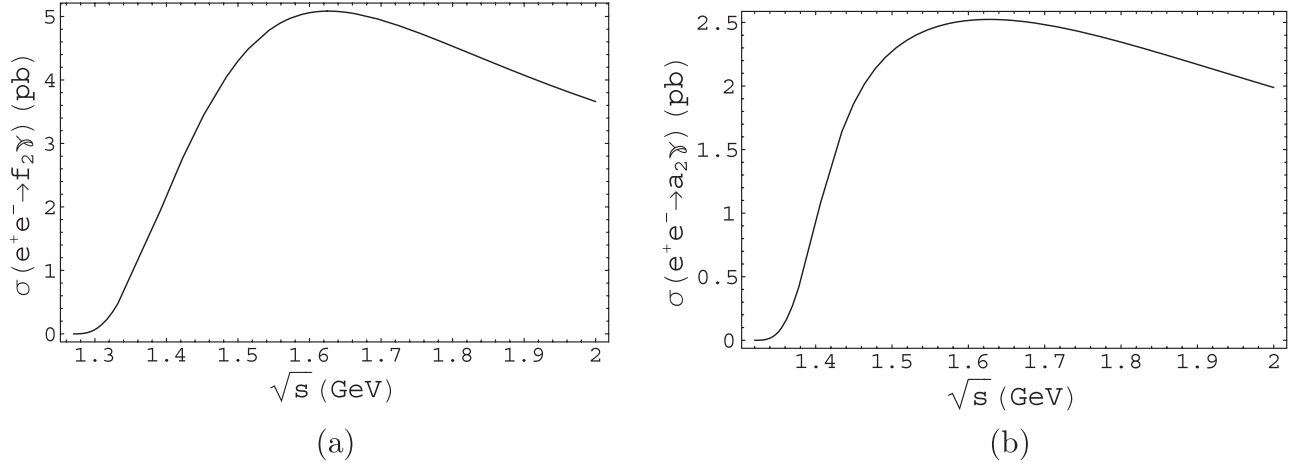


FIG. 2. (a) The $\sigma_{e^+e^- \rightarrow f_2\gamma}(s)$ for $g_{f_2\rho''\rho''} = g_{f_2\rho'\rho'} = g_{f_2\rho\rho}$. (b) The $\sigma_{e^+e^- \rightarrow a_2\gamma}(s)$ for $g_{a_2\rho''\omega''} = g_{a_2\rho'\omega'} = g_{a_2\rho\omega}$.

Assuming the VDM mechanism $e^+e^- \rightarrow (\rho + \rho' + \rho'') \rightarrow f_2(\rho + \rho' + \rho'') \rightarrow f_2\gamma$ one obtains

$$\sigma_{e^+e^- \rightarrow f_2\gamma}(s) = \frac{4\pi^2}{9} \alpha^3 \left(1 - \frac{m_{f_2}^2}{s}\right)^3 \left(\frac{s^2}{m_{f_2}^4} + 3\frac{s}{m_{f_2}^2} + 6\right) \times \left| \frac{m_\rho^2 g_{f_2\rho\rho}}{f_\rho^2 D_\rho(s)} + \frac{m_{\rho'}^2 g_{f_2\rho'\rho'}}{f_{\rho'}^2 D_{\rho'}(s)} + \frac{m_{\rho''}^2 g_{f_2\rho''\rho''}}{f_{\rho''}^2 D_{\rho''}(s)} \right|^2 \quad (9)$$

and

$$\Gamma_{f_2 \rightarrow \gamma\gamma} = \frac{\pi\alpha^2}{5} \left| \frac{g_{f_2\rho\rho}}{f_\rho^2} + \frac{g_{f_2\rho'\rho'}}{f_{\rho'}^2} + \frac{g_{f_2\rho''\rho''}}{f_{\rho''}^2} \right|^2 m_{f_2}^3 = 3.03 \pm 0.35 \text{ keV}, \quad (10)$$

Ref. [18]. We use the same parameters of the ρ , ρ' , ρ'' as for the $e^+e^- \rightarrow a_0\gamma$ and $e^+e^- \rightarrow f_0\gamma$ reactions. It is assumed that $g_{f_2\rho\rho}$ and other constants with crossed vector mesons are suppressed due to a small overlap of the spatial wave functions of ρ , ρ' and ρ'' . The f_V is obtained from the relation

$$\Gamma_{V \rightarrow e^+e^-}(s) = \frac{4\pi\alpha^2}{3f_V^2} \frac{m_V^4}{s^{3/2}}. \quad (11)$$

If one assumes that $g_{f_2\rho\rho} = g_{f_2\rho'\rho'} = g_{f_2\rho''\rho''}$, then Fig. 2(a) is obtained.

The $\pi^0\pi^0$ invariant mass m spectra is

$$\frac{d\sigma_{e^+e^- \rightarrow f_2\gamma \rightarrow \pi^0\pi^0\gamma}(s, m)}{dm} = \frac{8\pi}{9} \alpha^3 \left(1 - \frac{m^2}{s}\right)^3 \left(\frac{s^2}{m_{f_2}^4} + 3\frac{s}{m_{f_2}^2} + 6\right) \times \left| \frac{m_\rho^2 g_{f_2\rho\rho}}{f_\rho^2 D_\rho(s)} + \frac{m_{\rho'}^2 g_{f_2\rho'\rho'}}{f_{\rho'}^2 D_{\rho'}(s)} + \frac{m_{\rho''}^2 g_{f_2\rho''\rho''}}{f_{\rho''}^2 D_{\rho''}(s)} \right|^2 \times \frac{\Gamma_{f_2 \rightarrow \pi^0\pi^0}(m)^2}{|D_{f_2}(m)|^2}. \quad (12)$$

Using the $\Gamma_{f_2 \rightarrow \pi^0\pi^0}(m)$ and the inverse propagator $D_{f_2}(m)$ from the Appendix, one gets Fig. 3(a), where cutting ± 100 MeV around m_ω in the $\pi^0\gamma$ mass was done to reduce the $\omega\pi^0$ background, see also Sec. IV.

The photon angular distribution is

$$\frac{dn_\gamma^T}{d\Omega} = \frac{T}{N}, \quad (13)$$

$$T = \frac{(6m_{f_2}^4 + s^2)(1 + \cos^2\theta) + 6sm_{f_2}^2 \sin^2\theta}{3m_{f_2}^4}, \quad (14)$$

$$N = \frac{16\pi}{9} \left(\frac{s^2}{m_{f_2}^4} + 3\frac{s}{m_{f_2}^2} + 6\right). \quad (15)$$

The pion angular distribution in the rest frame of the tensor meson is

$$W_2(\vartheta, \varphi) = \frac{15}{16\pi} \left\{ \sin^4\vartheta \rho_{22} + \sin^2 2\vartheta \rho_{11} + 3\left(\cos^2\vartheta - \frac{1}{3}\right)^2 \rho_{00} + 2\cos\varphi \sin 2\vartheta \left(\sin^2\vartheta \rho_{21} - \sqrt{6}\left(\cos^2\vartheta - \frac{1}{3}\right)\rho_{10}\right) - 2\sqrt{6}\cos 2\varphi \sin^2\vartheta \left(\cos^2\vartheta - \frac{1}{3}\right)\rho_{20} \right\}. \quad (16)$$

Here the z axis is along the direction of the tensor meson momentum in the e^+e^- center-of-mass system, x is in the reaction plane and y is perpendicular to the reaction plane [19,20], ϑ is the polar angle and φ is the azimuthal angle.

After integration over φ one has

$$W_2(\vartheta) = \frac{15}{8} \left(\sin^4\vartheta \rho_{22} + \sin^2 2\vartheta \rho_{11} + 3\left(\cos^2\vartheta - \frac{1}{3}\right)^2 \rho_{00}\right). \quad (17)$$

For the $e^+e^- \rightarrow a_2\gamma$ we may use Lagrangians similar to Eqs. (7) and (8):

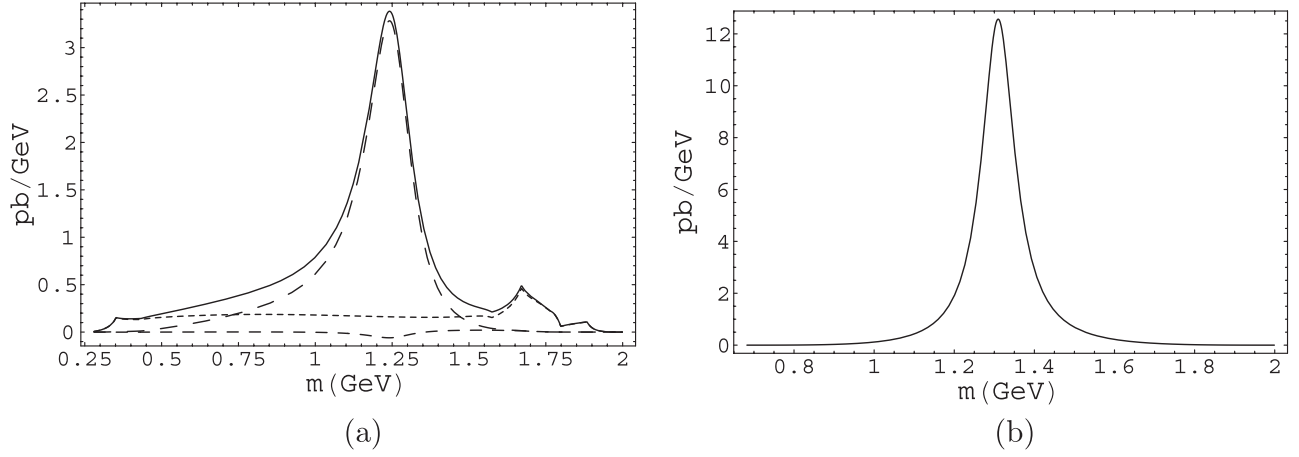


FIG. 3. (a) The $\pi^0\pi^0$ invariant mass spectra Eq. (12) in the reaction $e^+e^- \rightarrow \pi^0\pi^0\gamma$ for $g_{f_2\rho''\rho''} = g_{f_2\rho'\rho'} = g_{f_2\rho\rho}$ at $\sqrt{s} = 2$ GeV. Cuts of 100 MeV around the ω mass in $\pi^0(1)\gamma$ and $\pi^0(2)\gamma$ invariant masses have been applied. The solid line is the sum of the signal with cuts (long-dashed line) of the $\omega\pi^0$ background with cuts (short-dashed line) and of the interference (dashed line). (b) The $\eta\pi^0$ invariant mass spectra in the reaction $e^+e^- \rightarrow \eta\pi^0\gamma$ at $\sqrt{s} = 2$ GeV for $g_{a_2\omega''\rho''} = g_{a_2\omega'\rho'} = g_{a_2\omega\rho}$.

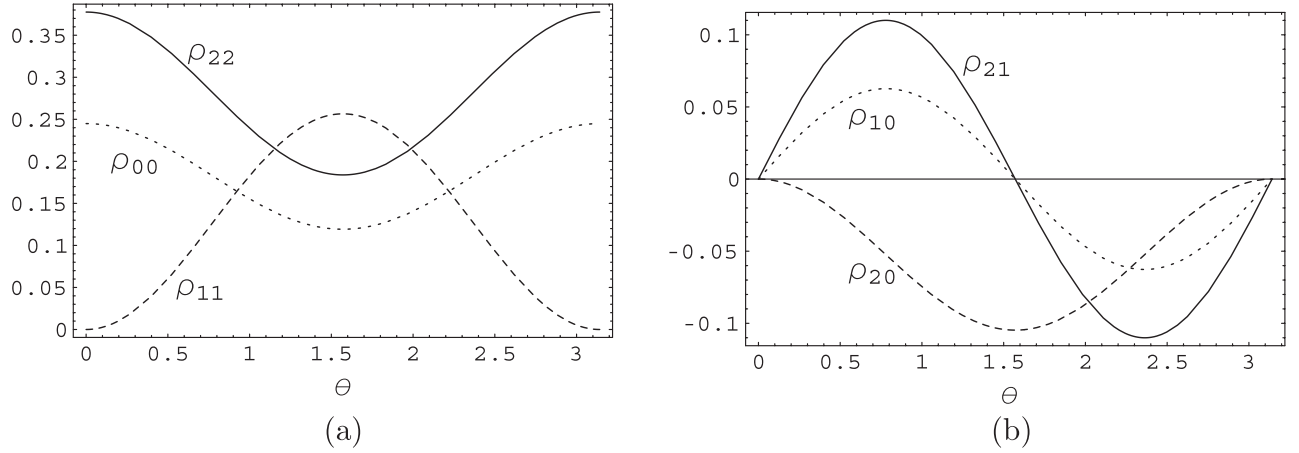


FIG. 4. The elements of the f_2 spin density matrix at $s = (1.5 \text{ GeV})^2$ (see Table I): (a) ρ_{22} (solid line), ρ_{11} (dashed line), ρ_{00} (short-dashed line); (b) ρ_{21} (solid line), ρ_{20} (dashed line), ρ_{10} (short-dashed line).

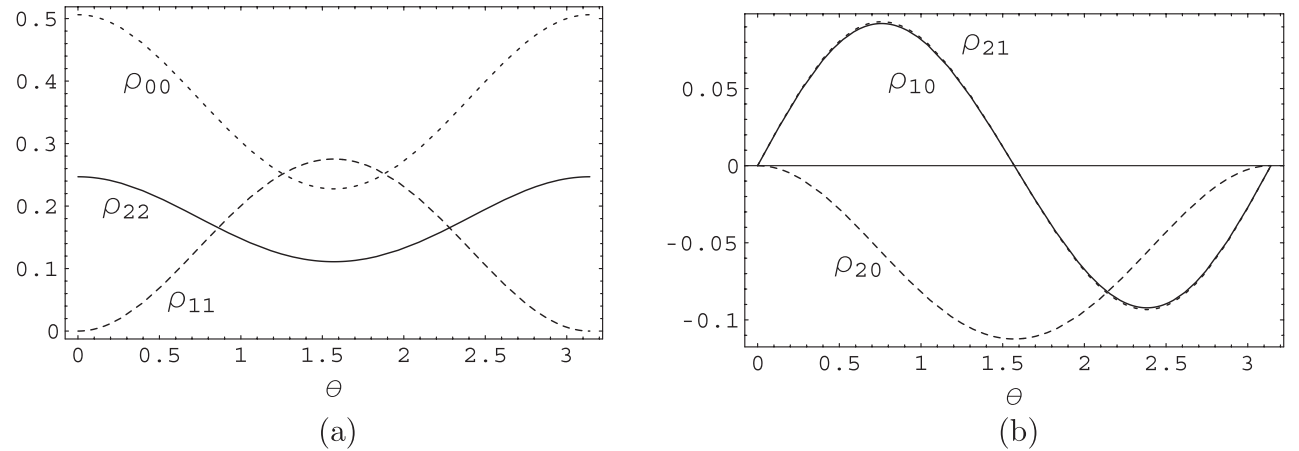


FIG. 5. As in Fig. 4 but for $s = (2 \text{ GeV})^2$.

$$L = g_{a_2\gamma\gamma} T_{\mu\nu} F_{\mu\sigma} F_{\nu\sigma}, \quad (18)$$

and

$$L = g_{a_2VV} T_{\mu\nu} F_{\mu\sigma}^V F_{\nu\sigma}^{V'}, \quad (19)$$

where $T_{\mu\nu}$ is the a_2 field, $V = \rho, \rho', \rho''$ and $V' = \omega, \omega', \omega''$.

Analogically one may write the $e^+e^- \rightarrow (\rho + \omega + \rho' + \omega' + \rho'' + \omega'') \rightarrow a_2(\omega + \rho + \omega' + \rho' + \omega'' + \rho'') \rightarrow a_2\gamma$ cross section neglecting $a_2\rho\omega'$, $a_2\rho'\omega$ and other cross vertices due to a small overlap of the spatial wave functions of ρ, ω' and ρ', ω and so on:

$$\begin{aligned} \sigma_{e^+e^- \rightarrow a_2\gamma}(s) &= \frac{\pi^2}{9} \alpha^3 \left(1 - \frac{m_{a_2}^2}{s}\right)^3 \left(\frac{s^2}{m_{a_2}^4} + 3\frac{s}{m_{a_2}^2} + 6\right) \\ &\times \left| \frac{m_\rho^2 g_{a_2\rho\omega}}{f_\rho f_\omega D_\rho(s)} + \frac{m_\omega^2 g_{a_2\rho\omega}}{f_\rho f_\omega D_\omega(s)} + \frac{m_{\rho'}^2 g_{a_2\rho'\omega'}}{f_{\rho'} f_{\omega'} D_{\rho'}(s)} \right. \\ &\left. + \frac{m_{\omega'}^2 g_{a_2\rho'\omega'}}{f_{\rho'} f_{\omega'} D_{\omega'}(s)} + \frac{m_{\rho''}^2 g_{a_2\rho''\omega''}}{f_{\rho''} f_{\omega''} D_{\rho''}(s)} + \frac{m_{\omega''}^2 g_{a_2\rho''\omega''}}{f_{\rho''} f_{\omega''} D_{\omega''}(s)} \right|^2, \end{aligned} \quad (20)$$

$$\begin{aligned} \Gamma_{a_2 \rightarrow \gamma\gamma} &= \frac{\pi\alpha^2}{5} \left| \frac{g_{a_2\rho\omega}}{f_\rho f_\omega} + \frac{g_{a_2\rho'\omega'}}{f_{\rho'} f_{\omega'}} + \frac{g_{a_2\rho''\omega''}}{f_{\rho''} f_{\omega''}} \right|^2 m_{a_2}^3 \\ &= 1.00 \pm 0.06 \text{ keV} \end{aligned} \quad (21)$$

Assuming $g_{a_2\rho''\omega''} = g_{a_2\rho'\omega'} = g_{a_2\rho\omega}$ gives Fig. 2(b) and $\eta\pi^0$ spectrum shown in Fig. 3(b). The angular distributions are the same as Eqs. (16) and (17) [with $m_{f_2} \rightarrow m_{a_2}$ substitution in Eqs. (14) and (15)].

IV. THE BACKGROUND SITUATION

Because of weakness of the signal cross sections in the region $1.4 \div 2$ GeV the background situation needs

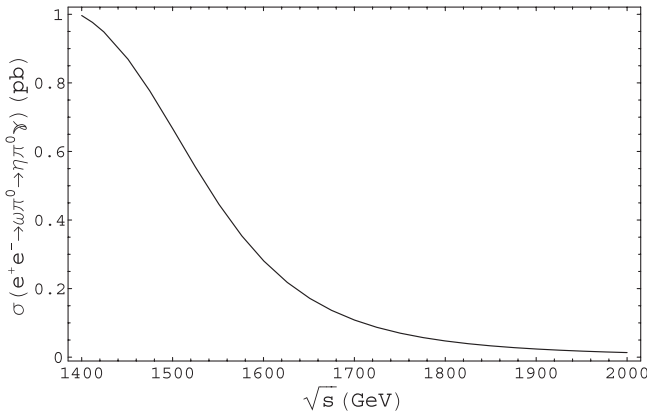


FIG. 6. The background cross section $\sigma_{e^+e^- \rightarrow \omega\pi^0 \rightarrow \eta\pi^0\gamma}(s)$ obtained with the help of Ref. [21].

TABLE I. Elements of the f_2 spin density matrix, see Figs. 4 and 5.

ρ_{22}	$\frac{1}{T}(1 + \cos^2\theta)$	ρ_{21}	$\frac{1}{T} \frac{\sqrt{s} \sin(2\theta)}{2m_{f_2}}$	ρ_{20}	$-\frac{1}{T} \frac{s \sin^2\theta}{\sqrt{6}m_{f_2}^2}$
ρ_{11}	$\frac{1}{T} \frac{s \sin^2\theta}{m_{f_2}^2}$	ρ_{10}	$\frac{1}{T} \frac{s^{3/2} \sin(2\theta)}{2\sqrt{6}m_{f_2}^3}$	$\rho_{1,-1}$	0
ρ_{00}	$\frac{1}{T} \frac{s^2(1+\cos^2\theta)}{3m_{f_2}^4}$	$\rho_{2,-1}$	0	$\rho_{2,-2}$	0

to be treated accurately. The $e^+e^- \rightarrow f_0\gamma \rightarrow \pi^0\pi^0\gamma$ and $e^+e^- \rightarrow a_0\gamma \rightarrow \eta\pi^0\gamma$ are expected to be too small to be observed themselves, but for $e^+e^- \rightarrow f_2\gamma \rightarrow \pi^0\pi^0\gamma$ and $e^+e^- \rightarrow a_2\gamma \rightarrow \eta\pi^0\gamma$ it is possible to reduce background to the level much less than the signal one.

The background situation in the case of $e^+e^- \rightarrow a_0\gamma \rightarrow \eta\pi^0\gamma$ and $e^+e^- \rightarrow a_2\gamma \rightarrow \eta\pi^0\gamma$ is rather easy to treat. The main background $e^+e^- \rightarrow \omega\pi^0 \rightarrow \eta\pi^0\gamma$ obtained with the help of Ref. [21] is much less than the signal cross section, see Figs. 2(b) and 6. Other backgrounds are even much smaller.

The main background in the case of $e^+e^- \rightarrow f_0\gamma \rightarrow \pi^0\pi^0\gamma$ and $e^+e^- \rightarrow f_2\gamma \rightarrow \pi^0\pi^0\gamma$ reactions comes from the $\omega\pi^0$ intermediate state also. Figure 3(a) shows that cut ± 100 MeV from the ω mass in the $\pi^0\gamma$ distribution reduces this background to the small level.

V. CONCLUSION

Our analysis shows that it should be possible to observe the reactions $e^+e^- \rightarrow a_2\gamma \rightarrow \eta\pi^0\gamma$ and $e^+e^- \rightarrow f_2\gamma \rightarrow \pi^0\pi^0\gamma$ at the energies near 2 GeV in VEPP-2000 after reaching the project luminosity and probably in DAΦNE after the planned full upgrade.

As to the reactions $e^+e^- \rightarrow a_0\gamma \rightarrow \eta\pi^0\gamma$ and $e^+e^- \rightarrow f_0\gamma \rightarrow \pi^0\pi^0\gamma$ at the energies 1.7–2 GeV, in the kaon loop model their cross sections are very small, while if the mere VDM (pointlike $V S \gamma$ interaction) was correct they would be observed, see Fig. 1. As it was shown in Ref. [22], the kaon loop mechanism gives arguments in favor of the four quark nature of light scalar mesons [23,24].

Of course, our calculations should be treated as a guide to prove the suppression of the scalar production in comparison to tensor one. Note that the $\pi^+\pi^-$ loop contribution in the scalar case, see, for example, [25,26], is small as shown in [25].

ACKNOWLEDGMENTS

We thank A. A. Kozhevnikov very much for useful discussions concerning $e^+e^- \rightarrow K^+K^-$ cross section drawn in Ref. [12]. This work was supported in part by RFBR, Grant No. 13-02-00039, and Interdisciplinary Project No. 102 of the Siberian division of RAS.

**APPENDIX: THE PROPAGATORS OF
THE $a_2(1320)$ AND $f_2(1270)$**

According to [27], we used the following inverse propagators for $T = a_2, f_2$:

$$D_T(m^2) = m_T^2 - m^2 - im\Gamma_T(m), \quad (\text{A1})$$

where

$$\begin{aligned} \Gamma_{a_2}(m) &= \Gamma_{a_2 \rightarrow \pi\pi}(m) \\ &= \Gamma_{a_2}^{\text{tot}} \frac{m_{a_2}^2}{m^2} \frac{p_{\eta\pi}^5(m)}{p_{\eta\pi}^5(m_{a_2})} \frac{D_2(r_{a_2} p_{\eta\pi}(m_{a_2}))}{D_2(r_{a_2} p_{\eta\pi}(m))}, \end{aligned} \quad (\text{A2})$$

and

$$\Gamma_{f_2}(m) = \Gamma_{f_2 \rightarrow \pi\pi}(m) + \Gamma_{f_2 \rightarrow K\bar{K}}(m) + \Gamma_{f_2 \rightarrow 4\pi}(m), \quad (\text{A3})$$

which is dominated by

$$\begin{aligned} \Gamma_{f_2 \rightarrow \pi\pi}(m) &= \Gamma_{f_2}^{\text{tot}} B(f_2 \rightarrow \pi\pi) \frac{m_{f_2}^2}{m^2} \frac{p_{\pi\pi}^5(m)}{p_{\pi\pi}^5(m_{f_2})} \\ &\times \frac{D_2(r_{f_2} p_{\pi\pi}(m_{f_2}))}{D_2(r_{f_2} p_{\pi\pi}(m))}. \end{aligned} \quad (\text{A4})$$

Here $D_2(x) = 9 + 3x^2 + x^4$ [28], and we take from Ref. [27] $m_{a_2} = 1322$ MeV, $\Gamma_{a_2}^{\text{tot}} = 116$ MeV, $r_{a_2} = 1.9$ GeV⁻¹, $m_{f_2} = 1272$ MeV, $\Gamma_{f_2}^{\text{tot}} = 196$ MeV, $B(f_2 \rightarrow \pi\pi) = 0.848$, $r_{f_2} = 8.2$ GeV⁻¹. The $\Gamma_{f_2 \rightarrow K\bar{K}}(m)$ has the similar form as Eq. (A4), we use $B(f_2 \rightarrow K\bar{K}) = 0.046$. The $\Gamma_{f_2 \rightarrow 4\pi}(m)$ may be approximated by the S-wave $f_2 \rightarrow \rho\rho \rightarrow 4\pi$ decay width as in Ref. [27], but for simplicity we used the dependence $\Gamma_{f_2 \rightarrow 4\pi}(m) = \Gamma_{f_2 \rightarrow 4\pi, m_{f_2}} \frac{m^2}{m_{f_2}^2}$ as in Ref. [29], here $B(f_2 \rightarrow 4\pi) = 0.106$.

-
- [1] N.N. Achasov and V.N. Ivanchenko, *Nucl. Phys.* **B315**, 465 (1989).
- [2] N.N. Achasov and V.V. Gubin, *Phys. Rev. D* **56**, 4084 (1997).
- [3] M.N. Achasov *et al.*, *Phys. Lett. B* **438**, 441 (1998); **440**, 442 (1998); **479**, 53 (2000); **485**, 349 (2000).
- [4] R.R. Akhmetshin *et al.* (CMD-2 Collaboration), *Phys. Lett. B* **462**, 380 (1999).
- [5] A. Aloisio *et al.* (KLOE Collaboration), *Phys. Lett. B* **536**, 209 (2002).
- [6] A. Aloisio *et al.* (KLOE Collaboration), *Phys. Lett. B* **537**, 21 (2002); C. Bini, P. Gauzzi, S. Giovannella, D. Leone, and S. Miscetti, KLOE Note No. 173 06/02, <http://www.lnf.infn.it/kloe/>.
- [7] N.N. Achasov and V.V. Gubin, *Phys. Rev. D* **63**, 094007 (2001).
- [8] N.N. Achasov, *Nucl. Phys.* **A728**, 425 (2003).
- [9] N.N. Achasov and A.V. Kiselev, *Phys. Rev. D* **68**, 014006 (2003).
- [10] N.N. Achasov and A.V. Kiselev, *Phys. Rev. D* **73**, 054029 (2006); **74**, 059902(E) (2006); *Yad. Fiz.* **70**, 2005 (2007) [*Phys. At. Nucl.* **70**, 1956 (2007)].
- [11] N.N. Achasov and A.V. Kiselev, *Phys. Rev. D* **83**, 054008 (2011); **85**, 094016 (2012).
- [12] N.N. Achasov and A.A. Kozhevnikov, *Phys. Rev. D* **57**, 4334 (1998).
- [13] The mere VDM prediction is obtained by the removal of the loop integral $\bar{g}(m)$ in Eqs. (1) and (2) and normalization of the cross section on the signal one at $\sqrt{s} = m_\phi$.
- [14] P.M. Ivanov, L.M. Kurdadze, M. Yu. Lelchuk, V.A. Sidorov, A.N. Skrinsky, A.G. Chilingarov, Yu.M. Shatunov, B.A. Shwartz, and S.I. Eidelman (OLYA Collaboration), *Phys. Lett.* **107B**, 297 (1981).
- [15] D. Bisello *et al.* (DM2 Collaboration), *Z. Phys. C* **39**, 13 (1988).
- [16] N.N. Achasov, *Phys. Lett. B* **222**, 139 (1989).
- [17] N.N. Achasov and V.A. Karnakov, *Z. Phys. C* **30**, 141 (1986).
- [18] J. Beringer *et al.* (Particle Data Group) *Phys. Rev. D* **86**, 010001 (2012).
- [19] K. Gottfried and J.D. Jackson, *Nuovo Cimento* **33**, 309 (1964).
- [20] J.D. Jackson, *Nuovo Cimento* **34**, 1644 (1964).
- [21] N.N. Achasov and A.A. Kozhevnikov, *Phys. Rev. D* **55**, 2663 (1997).
- [22] N.N. Achasov, *Nucl. Phys.* **A728**, 425 (2003); *Yad. Fiz.* **67**, 1552 (2004) [*Phys. At. Nucl.* **67**, 1529 (2004)].
- [23] R.L. Jaffe, *Phys. Rev. D* **15**, 267 (1977); **15**, 281 (1977).
- [24] N.N. Achasov, S.A. Devyanin, and G.N. Shestakov, *Z. Phys. C* **22**, 53 (1984).
- [25] N.N. Achasov and G.N. Shestakov, *Phys. Rev. D* **77**, 074020 (2008).
- [26] S. Eidelman, S. Ivashyn, A. Korchin, G. Pancheri, and O. Shekhovtsova, *Eur. Phys. J. C* **69**, 103 (2010).
- [27] N.N. Achasov, G.N. Shestakov, *Usp. Fiz. Nauk* **181**, 827 (2011) [*Phys. Usp.* **54**, 799 (2011)].
- [28] J.M. Blatt and V.F. Weisskopf, *Theoretical Nuclear Physics* (Wiley, New York, 1952), pp. 359–365 and 386–389.
- [29] S. Uehara *et al.* (Belle Collaboration), *Phys. Rev. D* **82**, 114031 (2010).